CEST IMAGING WITH ALTERNATING-OFFSET-SATURATION BSSFP

Qi Liu[1,2], Zhaoyang Fan[2], Wafa Tawackoli[2], Gadi Pelled[2], Dan Gazit[2], Yutaka Natsuaki[3], and Debiao Li[2,4]

[1]*Northwestern University, Chicago, IL, United States,* [2]*Cedars-Sinai Medical Center, Los Angeles, CA, United States,* [3]*Siemens Healthcare, Los Angeles, CA,*

[4]*University of California, Los Angeles, CA, United States*

Introduction:

By probing proton chemical exchange between bulk-water and endogenous or exogeneous solutes, chemical exchange saturation transfer (CEST) imaging can reveal information on compound concentration, tissue pH, and temperature [1]. On clinical scanners CEST is commonly performed by preparing the magnetization by a number of long-duration, high-power saturation pulses before the imaging sequence, interleaved by spoiling gradients. Typically a so-called Z-spectrum is generated by imaging with varied saturation pulse frquency offsets, starting at the lowest (or the highest) offset and gradually increasing (or decreasing) to the highest (or the lowest) offset, resulting in long imaging time. Meanwhile, endogeneous CEST effect is usually small, requiring high signal-to-noise ratio (SNR) for accurate detection. Balanced steady-state-free-precession (bSSFP) allows rapid imaging with SNR efficiency [2] as compared to conventional turbo spin-echo (TSE) acquisition. However, bSSFP is sensitive to field inhomogeneties and scanner frequency drift. In this study, we developed an alternating-offset-saturation bSSFP (AOS-bSSFP) technique for more accurate CEST detection, as demonstrated by excellent agreement with TSE CEST in MTR_{asym} plot both in phantom and *in vivo* scans.

Methods:

Water resonance frequency was measured by a TSE-based, WASSR-like method [3], which was repeated several times to demonstrate scanner frequency drift. All scans were performed at a same slice, with same CEST saturation scheme except the order of saturation offset. AOS-bSSFP had the same imaging parameters as conventional-bSSFP (C-bSSFP), and was acquired with alternating CEST saturation frequency offsets, eg: -6 ppm, +6 ppm, -5.5 ppm, +5.5 ppm,….C-bSSFP and TSE were acquired with conventional linear increasing CEST saturation frequency offsets, eg: -6 ppm, -5.5 ppm, -5 ppm, -4.5 ppm, …

Data acquisition: All studies were conducted on a 3.0T system (Verio, Siemens). Manual shimming was performed at the beginning. The WASSR-like method was used to assess the amount of scanner frequency drift: 13 images were acquired with evenly distributed offsets between -1 ppm and +1 ppm, using one 90°, 40ms Gaussian saturation. For phantom/*in vivo* CEST scans, saturation consists of a train of 10/24 Gaussian pulses with flip angle of 1800°/2400°, 90ms duration, 50% duty cycle, and interleaved by spoiling gradients. For phantom studies, a tube of 15 g/L creatine solution inside a larger tube of water was imaged with body matrix coils. FOV was 160×160 mm^2. Resolutions were 1.0×1.0 mm^2 for bSSFP and 1.25×1.25 mm^2 for TSE. 41 images with offsets distributed evenly between -9ppm and +9ppm, and one S0 image (image with no satuation) were acquired. 5 healthy volunteers (age 25.2 ± 0.8 years) participated in *in vivo* study. A 5mm axial slice in the brain was imaged with 8-channel head coils. FOV was 210×210 mm^2. Resolutions were 1.31×1.31 mm^2 for bSSFP and 1.64×1.64 mm^2 for TSE. 25 images with offsets distributed evenly between -6ppm and +6ppm, two additional offsets at -20ppm and +20ppm, and one S0 image were acquired. Other parameters for bSSFP were: 10 dummy pulses, flip angle 70°, TR 5000ms, echo-spacing 3.4 ms, centric-reordering, 3 shots per slice. Other parameters for TSE were: TE 19ms, TR 5000ms, echo train length 47, flip angle 180°. Acquisition times were 6.2 and 8.3 mins for bSSFP and TSE, respectively.

Data analysis: All images were first interpolated to a same matrix size and normalized by its corresponding B0 image. Then on a pixel-by-pixel basis, location of water peak was determined by fitting Z-spectrum with a Lorentzen function at data points from -1ppm to 1ppm, and from -2.5ppm to 0.5ppm, for WASSR-like and CEST scans respectively. Next, based on this information B0 inhomogeneity was corrected. MTR_{asym} were calculated by subtracting CEST signal of positive offset from negative offset. In each volunteer, one ROI spanning at least 150 pixels was drawn in a homogeneous white matter region which was susceptible to frequency drift as indicated on field-map. Then Z-spectrum data was averaged within the ROI. To assess the agreement between two Z-spectra, the root-mean-square (RMS) value of the difference curve is calculated over all offsets. Paired-t test at α=0.05 was used to test the RMS between C-bSSFP & TSE ($RMS_{c\text{-}bSSFP\&TSE}$) and RMS between AOS-bSSFP & TSE ($RMS_{AOS\text{-}bSSFP\&TSE}$).

Results:

Scanner frequency drift on phantom and human brain is shown by field-map at different time points, as in Figure 1. Typical drifts are: 0.4 ppm in the phantom study in 60 mins, and 0.15 ppm in one human brain study in 45 mins. Clearly for long imaging time scans such as CEST, the problem of scanner frequency drift should be considered. Typical MTR_{asym} of the creatine phantom and human brain are plotted in Figure 2: C-bSSFP plot significantly deviates from TSE, while the proposed AOS-bSSFP has better agreement. Paired t-test also shows that the proposed AOS-bSSFP method has significantly better agreement with TSE than the conventional method, as $RMS_{AOS\text{-}bSSFP\&TSE}$ (0.0051 ± 0.0008) is lower than $RMS_{c\text{-}bSSFP\&TSE}$ (0.0091 ± 0.0024) , with p=0.011.

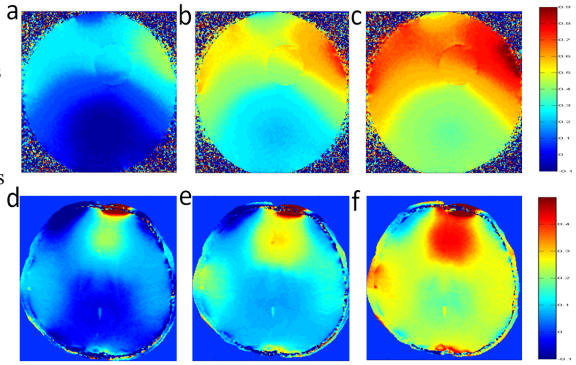

Fig 1. Phantom field map at t = 0 (a), 30 mins (b), 60 mins (c), shown with the same colorbar (in ppm). Volunteer brain field map at t = 0 (d), 26 mins (e), 45 mins (f), shown with the same colorbar (in ppm). Typical drift between (c) and (a) is 0.4 ppm, between (d) and (f) is 0.15 ppm.

Discussion and Conclusions:

We have successfully achieved *ex vivo* and *in vivo* CEST imaging using the proposed AOS-bSSFP acquisition scheme. bSSFP acquisition is sensitive to scanner frequency drift, which causes inaccurate MTR_{asym} measurement in C-bSSFP. Under the hypothesis that frequency drift is a relative slow process, the proposed technique can minimize frequency change between the positive and negative offset in Z-spectrum, thus leads to more accurate MTR_{asym}, serving the foundation for further analysis. To the best of our knowledge, this is the first time bSSFP has been used on CEST imaging *in vivo*.

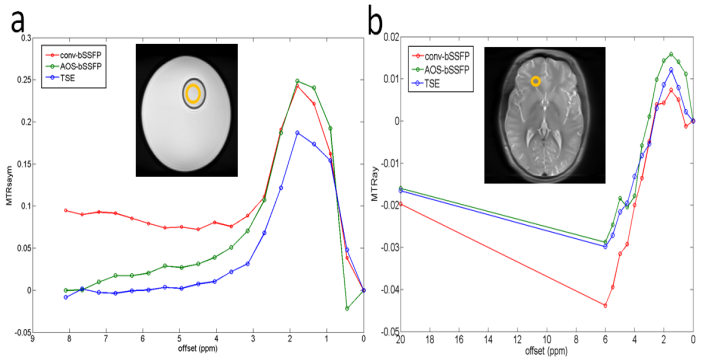

Fig 2. Typical MTRasym plot for creatine phantom (a) and human brain (b) across all methods.

References: [1] MRM (20011); 65: 927-948 [2] Eur Radiol (2003); 13 : 2409-2418

[3] MRM (2009); 61: 1441-1450